HHS Public Access

Author manuscript

Nat Commun. Author manuscript; available in PMC 2013 September 10.

Published in final edited form as:

Nat Commun. 2013 ; 4: 1449. doi:10.1038/ncomms2438.

Genome-wide profiles of CtBP link metabolism with genome stability and epithelial reprogramming in breast cancer

Li-Jun Di[1], **Jung S. Byun**[1], **Madeline M. Wong**[1], **Clay Wakano**[1], **Tara Taylor**[1], **Sven Bilke**[1], **Songjoon Baek**[2], **Kent Hunter**[3], **Howard Yang**[4], **Maxwell Lee**[4], **Celia Zvosec**[5], **Galina Khramtsova**[5], **Fan Cheng**[6], **Charles M. Perou**[6], **C. Ryan Miller**[6], **Rachel Raab**[7], **Olufunmilayo I. Olopade**[5], and **Kevin Gardner**[1,8]

[1]Genetics Branch, National Cancer Institute, Bethesda, Maryland, 20892, USA

[2]Laboratory of Receptor Biology and Gene Expression, National Cancer Institute, Bethesda, Maryland, 20892, USA

[3]Laboratory of Cancer Biology and Genetics, National Cancer Institute, Bethesda, Maryland 20892, USA

[4]Laboratory of Population Genetics, National Cancer Institute, Bethesda, Maryland, 20892, USA

[5]Department of Medicine, University of Chicago, Chicago, IL, 60637, USA

[6]Lineberger Comprehensive Cancer Care Center, University of North Carolina, Chapel Hill, 27599, USA

[7]Leo W. Jenkins Cancer Center, East Carolina University, Greenville North Carolina, 27834, USA

Abstract

The C-terminal binding protein (CtBP) is a NADH-dependent transcriptional repressor that links carbohydrate metabolism to epigenetic regulation by recruiting diverse histone modifying complexes to chromatin. Here, global profiling of CtBP in breast cancer cells reveals that it drives epithelial to mesenchymal transition, stem cell pathways, and genome instability. CtBP expression induces mesenchymal and stem cell-like features while CtBP depletion or caloric restriction

[8]Corresponding author: 41 Library Drive, Bldg 41/D305, Bethesda, MD 20892-5065, (301) 496-1055, gardnerk@mail.nih.gov.

Author contributions

L-J.D. performed most of the experiments generated data and figures and co-wrote the manuscript. J.S.B. performed experiments and generated data and figures and co-wrote the manuscript. M.M.W. performed experiments and generated data. C.W. performed experiments. T.T. generated and analyzed data. S.B. analyzed data and generated figures. S.B. generated methods and analyzed data. K.H. analyzed data. H.Y. generated methods and analyzed data. M.L. generated methods and analyzed data. C.Z. collected clinical information and analyzed data. G.K. collected clinical information and analyzed data. F.C. generated methods, analyzed data and generated figures. C.M.P. generated methods, analyzed data and generated figures. C.R.M. analyzed data. R.R. collected clinical information and analyzed data. O.I.O. collected clinical information and analyzed data. K.G. designed study, supervised the study, analyzed data, and co-wrote the manuscript.

Competing Financial Interest

C.M.P is an equity stock holder of BioClassifier LLC and University Genomics. C.M.P. has also filed a patent on the PAM50 assay ("GENE EXPRESSION PROFILES TO PREDICT BREAST CANCER OUTCOMES", US Patent Application 20110145176). All other authors declare no competing financial interests.

Accession codes

Microarray data have been deposited in the Gene Expression Omnibus database under series accession code GSE36529.

reverses gene repression and increases DNA repair. Multiple members of the CtBP-targeted gene network are selectively down-regulated in aggressive breast cancer subtypes. Differential expression of CtBP-targeted genes predicts poor clinical outcome in breast cancer patients, and elevated levels of CtBP in patient tumors predict shorter median survival. Finally, both CtBP promoter targeting and gene repression can be reversed by small molecule inhibition. These findings define broad roles for CtBP in breast cancer biology and suggest novel chromatin-based strategies for pharmacologic and metabolic intervention in cancer.

Introduction

Cancer evolves through a multi-step process driven by a global reprogramming of cellular gene expression patterns that confers adaptive advantages for tumor growth, proliferation and dissemination [1]. This phenotypic transformation is accomplished by diverse molecular strategies that control programs of cellular function by directing large-scale changes in gene expression [2]. Although our understanding of how specific genetic mutations can act as drivers of cancer is well established, the paradigms addressing how epigenetic changes are orchestrated to influence hallmarks of cellular malignancy are only just beginning to evolve [3]. Epigenetic changes represent potentially reversible covalent modifications to chromatin that can be transmitted to subsequent generations in the absence of changes to genetic sequence. In combination with DNA methylation, and histone modifications (including acetylation, methylation, phosphorylation and ubiquitylation), these covalent modifications constitute a “histone code” that is sculpted and interpreted by an assortment of chromatin regulatory complexes that bind (“read”), place (“write”), and remove (“erase”) chromatin marks to create the living “libretto” that we now refer to as the ‘epigenome’ [3]. How the spatial and kinetic distribution of these chromatin regulatory complexes are coordinated to influence the epigenome has become the focus of extensive investigation [4].

The C-terminal binding proteins (CtBP1/2) are a dimeric family of proteins encoded by two paralogous genes, *CtBP1* and *CtBP2*, that play extensive roles in animal cell development [5]. CtBP homo- and hetero-dimerize in the presence of NADH to recruit various chromatin modifying complexes, including histone methyl-transferases (HMTs), histone demethylases (HDMs), and histone deacetylases (HDACs) (e.g LSD1, HDAC1/2/4/6/7, G9a and EHMT) to chromatin bound sequence-specific transcription factors [5]. In this way, CtBP has the potential to link metabolic status to specific changes in the epigenetic landscape of the nucleus and play a dominant role in determining cellular behavior and fate [6, 7]. However, with the exception of a small set of tumor suppressor genes (e.g. *CDH1* (*E-Cadherin*), *CDKN2A* (*p16*), *Sirtuin 1* and *BRCA1*) [6, 8], the genome-wide targets of CtBP in the mammalian nucleus remain unknown.

Previously we showed that CtBP repressed the transcriptional expression of the early onset breast cancer gene, *BRCA1*, by recruiting HDAC activity to the *BRCA1* promoter to antagonize p300 driven histone acetylation [8]. In this current work we extend this observation by profiling the global association of CtBP with the genome of breast cancer cells by combining chromatin immunoprecipitation with deep sequencing (ChIP-Seq) to define cellular programs driven by CtBP with clinical importance, and potential for therapeutic

targeting. Here we reveal that CtBP plays a prominent role in epigenetic reprogramming that drives major hallmarks of cancer through transcriptional mechanisms that are both linked to metabolism and susceptible to pharmacologic intervention.

Results

CtBP targets cellular reprograming and genome stability

Recent molecular and morphological studies have shown that most breast cancers can be separated into distinct subtypes that segregate along the hierarchy of normal mammary epithelial differentiation and development and include, luminal A, luminal B, human epithelial growth factor receptor 2 (HER2) positive, basal-like, and claudin low [9, 10]. Luminal A and B are well-differentiated tumors and usually estrogen receptor positive. The basal-like and claudin low subtypes are much more primitive and usually deficient in receptors for estrogen and progesterone and HER2 [9, 10]. This classification has substantial diagnostic and prognostic importance. The more primitive tumors (e.g. basal-like and claudin low) usually show a more aggressive behavior with worse clinical outcome [9, 10]. Properties of these tumors include mesenchymal features associated with reactivation of embryonic programs that promote epithelial to mesenchymal transition (EMT), acquisition of stem cell-like self-renewal attributes, increased genome instability, and the production of cellular progenitors with the ability to seed new tumors, often referred to as “tumor initiating cells” (TICs) [1112, 13]. Such features are recognized as important hallmarks or drivers of cancer [1].

We profiled the binding of CtBP across the genome of the human breast cancer cell line MCF-7, a well differentiated estrogen receptor positive luminal subtype, using antibodies that recognize epitopes common to both CtBP1 and CtBP2 (Fig. 1). Genome wide ChIP-seq analysis identified a total of 6607 binding sites for CtBP with a FDR<0.00001. 1823 of these binding sites were in promoter regions (Table 1). Consistent with the established role for CtBP in animal cell development [14], ontology analysis of the 1823 gene promoters demonstrates that CtBP interacts with gene networks that have broad roles in cellular homeostasis including cellular macromolecule metabolic processes, RNA processing, gene expression, and cellular metabolic processes (Supplementary Table S1). However, a large number of CtBP targeted genes belong to categories that are important in malignant tumor transformation and progression, including embryonic development, cellular response to DNA damage, cell cycle, cell proliferation, cell death, cell adhesion and chromatin modifications (Fig. 1a). CtBP binding sites located outside of promoter regions are also nearby genes that show a similar distribution of these categories (Supplementary Figs. S1a–d). In particular, many of the CtBP target genes belong to functional gene categories that play major roles in driving the more aggressive mesenchymal phenotypes of basal-like and claudin low tumors including genome instability, EMT, and stem cell-like/tumor initiating cell (TIC) pathways [10, 13] (Fig. 1b). The core list of 30 CtBP bound genes in Figure 1b (10 from each category, each with Z-scores > 30.17), include multiple genes that have been previously shown to play major roles in breast cancer etiology, genetic susceptibility and tumor progression [15, 16]. It was therefore selected for use in subsequent validation studies.

In silico analysis of consensus binding motifs centered under CtBP peaks shows a large enrichment of transcription factor binding sites (TFBS) for ETS, CREB, STAT and EGR1/SP1 families of transcription factors (Fig. 1c and Supplementary Fig. S2). Notably, these motifs are over-represented in the promoters of both bi-directional and DNA repair genes including *BRCA1, PALB2, FANCD2, FANCM* and *RAD51C* [17, 18] (also see Fig. 1b). In addition, the ETS-pathway has been identified as a major program in basal-like breast cancers [19]. This finding suggests that CtBP recruitment is likely to be coordinated through a common promoter context to control specific cellular programs.

CtBP is often found in complexes with the histone demethylase, LSD1, where it plays a broad role in both repressive and activating transcriptional programs in various cell types [20–22]. In breast epithelia, LSD1 represses invasion and metastasis [23]. However, comparison of the targets of CtBP and LSD1 in MCF-7 and human ES cells reveals less than a 7% and 10% overlap, respectively (Fig. 1d). This indicates that the major functions of CtBP in epigenetic regulation are likely to involve complexes that are distinct from LSD1 targeting in mammary epithelial cells.

CtBP promotes EMT and enhances tumor initiating cell traits

Though CtBP predominantly produces repression of target genes, both the dimeric state of CtBP and composition of the CtBP-containing complex are major determinants of whether CtBP will repress or induce gene expression [21, 24, 25]. An analysis of the relative enrichment of CtBP targeted genes in molecular signatures of EMT [26] shows a significant (P=9.5 E-11) overlap with genes that are differentially repressed (down-regulated) compared to activated (up-regulated) during EMT (Fig. 2a). Similarly, CtBP bound genes are significantly more enriched (P=7.37E-10) in the genes that are differentially repressed in the cancer TIC/Stem cell signature [12] (Fig. 2a). These findings implicate a predominant role for CtBP in driving both EMT and stem cell-like attributes through transcriptional repression.

To obtain a general impression of the correlation between CtBP promoter occupancy and gene expression, microarray analysis was used to compare gene expression patterns in control versus MCF-7 cells that had been depleted of CtBP by RNAi (Fig. 2b). This screen identified 1585 genes that showed significant ($P< 0.05$) up-regulation and 1248 genes that showed down regulation by either direct or indirect CtBP influence. Using the FDR cutoff described above, 179 of the up-regulated and 100 of the down-regulated genes were identified as CtBP targets by ChIP-seq. Although the specific functional distribution of differentially expressed gene classes is similar to the ChIP-seq distribution shown in Figure 1a (Supplementary Fig. S7), the modest size of the overlap is likely a reflection of direct and indirect influences of CtBP depletion in combination with the insensitivity and low dynamic range of hybridization-based array technology [27]. Therefore, to generate a more accurate view of the relationship between CtBP occupancy and gene expression, a total of 71 genes (30 genes from Figure 1b and 41 additional genes collected from gene categories described in Figure 1; in total representing 26% of the EMT overlap and 38% of the TIC overlap in Figure 2a) were selected for validation by quantitative mRNA expression (qRT-PCR) and quantitative chromatin immunoprecipitation. Both cells depleted of CtBP by RNAi and cells over-expressing CtBP were analyzed and compared (Fig. 2c and Supplementary Figs. S3–

S6). By this analysis, 56% of the validation genes showed significant (P<0.05) up-regulation following CtBP depletion while 14% showed down-regulation (Supplementary Figs. S4–S6). Conversely, 46% of genes in cells over-expressing CtBP showed significant repression (P<0.05) while 15% showed upregulation. 100% of genes tested by quantitative ChIP showed a significant peak (P<0.05) and 90% (27 of 30) genes showed a significant decrease (P<0.05) of CtBP binding following CtBP gene depletion by RNAi (Supplementary Figs. S3 and S6). These data show that many of the genes identified by ChIP-seq analysis are likely to be bona fide functional targets of CtBP.

Global depletion of CtBP increases DNA repair

CtBP bound sequences are enriched in transcription factor binding sites found in the promoters of genes involved in DNA repair (Fig. 1b–c). Many of these are derepressed following CtBP depletion (Fig. 2c and Supplementary Fig. S4). These findings, in combination with the previously reported repressive effects of CtBP on BRCA1 expression [8], suggests that CtBP levels may have a strong influence on DNA repair. To test this, comet assays were performed on MCF-7 cells exposed to oxidative DNA damage before or after CtBP gene depletion by RNAi (Fig. 2d). Analysis reveals that cells depleted of CtBP show significantly increased DNA repair (P=6.0 E-09) compared to control cells (Fig. 2e). In contrast, gene depletion of BRCA1 by RNAi has the opposite effect (decreased DNA repair), though with lower relative significance (P=1.50 E-05) (Supplementary Fig. S8). These findings establish a substantial role for CtBP in governing transcriptional programs that control genome stability.

CtBP drives acquisition of mesenchymal traits

To assess the functional influence of CtBP on the acquisition of mesenchymal traits, we compared the effect of CtBP expression on the properties of two cell lines at opposite poles of the hierarchy of mammary differentiation (Fig. 3). MCF-7 cells serve as a representative of luminal differentiation while MDA-MB-231, an estrogen receptor negative and highly metastatic cell line, is representative of the claudin low subtype. In both cell lines CtBP depletion induces derepression of most of the 30 CtBP-targeted genes in Figure 1b, however gene depletion seems to derepress a substantially larger portion of the MDA-MB-231 cells than the MCF-7 (80% versus 53%) (Figs. 3a–b and Supplementary Fig S4). In contrast, CtBP over-expression has a more substantial influence on the repression of the 30 CtBP targets in MCF-7 compared to MDA-MB-231 (43% versus 6%) (Figs. 3a–b and Supplementary Fig S5). CtBP is associated with a variety of chromatin modifying complexes [5]. At the *BRCA1* promoter, loss of CtBP results in increased *BRCA1* promoter acetylation and increased *BRCA1* expression [8]. However, in the absence of direct empirical information or further study of the specific forms of CtBP complexes in different cell types or knowledge of the differential promoter recruitment of HATs, HDACs, HMTs, and HDMs, it is not possible to readily predict what modifications will be altered and in what direction at each individual CtBP target. Regardless, CtBP gene depletion produces substantial changes in both H3 and H4 histone acetylation at most of the 30 CtBP gene targets (Fig. 3c and Supplementary Fig. S9).

A well characterized attribute of the acquisition of mesenchymal features and EMT is increasing *vimentin* expression accompanied by decreasing *E-cadherin* expression [11]. To profile the influence of CtBP on these properties, the change in the *E-cadherin/Vimentin* ratio [28] was measured (Fig. 3d). In both MCF-7 cells and MDA-MB-231 cells, CtBP gene depletion increased the ratio of E-cadherin/Vimentin while CtBP expression lowered it, consistent with the ability of CtBP to drive the mesenchymal phenotype in both mesenchymal and luminal cells. Furthermore, the role of CtBP in driving mesenchymal features is well illustrated by the ability of enforced CtBP expression to substantially increase MCF-7 mobility in wound healing assays (Fig. 3e).

EMT has recently been shown to activate programs that promote the acquisition of stem cell-like properties [11]. This often occurs in progenitor cells with increases in *CD44* as opposed to *CD24* expression [11]. The influence of CtBP on stem-like features of MCF-7 and MDA-MB-231 was measured by profiling changes in the *CD44/CD24* ratio [10] following enforced CtBP expression or CtBP gene depletion (Fig. 3f). In both cell lines, expression of CtBP increased the *CD44/CD24* ratio consistent with the attributes of cells with progenitor/stem cell-like features, while CtBP depletion decreased that ratio (Fig. 3f). Thus CtBP appears to be able to drive the mesenchymal phenotype in mammary cells regardless of what position they are along the spectrum of mammary differentiation.

CtBP links cellular metabolic status to genome stability

Pharmacological manipulation of endogenous NADH levels influences *BRCA1* expression through CtBP, with higher levels of NADH causing *BRCA1* repression [8]. To ask whether manipulation of endogenous NADH levels by carbohydrate over-loading could influence expression of CtBP-targets, we grew MCF-7 cells in high or “diabetic” levels of glucose (450 mg/dl) versus normal concentration (100 mg/dl) (Fig. 4). CtBP dimerization, nuclear localization, and stability are enhanced when bound to NADH [7, 29]. As demonstrated by both immuno-histochemistry and Western blot analysis, MCF-7 cells grown in low levels of glucose, demonstrate decreased levels of NADH relative to NAD+, and show lower nuclear accumulation of CtBP in comparison to cells grown under conditions of high glucose (Figs. 4a–c). These changes are, in turn, associated with increased nuclear levels of BRCA1 protein, decreased levels of CtBP loading at the *BRCA1* promoter, compensatory increases in relative histone 3 acetylation [8] (Figs. 4c–e and Supplementary Fig. S10a); and a significant increase in the expression of *BRCA1* mRNA and other CtBP-targeted genes important in DNA repair (Fig. 4f and Supplementary Fig. S10b). Finally, as predicted, cells incubated under high glucose condition show a demonstrably reduced DNA repair capacity that is not due to differences in cell cycle entry (Figs. 4g–h and Supplementary Fig. S10c).

CtBP gene networks distinguish aggressive breast cancer

The embryonic properties linked to EMT, including cellular plasticity, dedifferentiation, de-regulated cell growth, and genome instability, are common features associated with more aggressive molecular subtypes of breast cancer [30, 31]. To ask whether CtBP-target genes define networks that are more associated with aggressive subtypes of breast cancer, we profiled the expression of CtBP target genes in publically available breast cancer patient gene expression data sets (Fig. 5a). Analysis by unsupervised hierarchical clustering

identified a large class or cluster of CtBP-targeted genes that are selectively downregulated in the basal-like and claudin low subtype of cancers (Fig. 5a). Moreover, ANOVA analysis [10] of expression of the CtBP-targeted gene categories (Fig. 1b), shows that down regulation of many of the genes within the EMT and Stem Cell/TIC categories significantly distinguish (P-values between 1.08E-11 and 1.17 E-140) basal-like and claudin low from the other subtypes (Fig. 5b and Supplementary Fig. S11). *GRHL2* has recently been shown to play a dominant role in EMT by regulating cell polarity and is a strong discriminator of claudin low subtypes [32, 33]. *FOXA1* potently distinguishes basal-like and claudin low from the more luminal subtypes and has recently been shown to actively repress the basal-like phenotype [34, 35] (Figs. 1b, 5b and Supplementary Fig. S11). Similarly, gene set enrichment analysis (GSEA) [36] of the genes altered by *CtBP* RNAi depletion using micro-array analysis (Fig. 2b) also reveals substantial CtBP dependent participation in multiple pathways important in breast cancer biology (Supplementary Figs. S12a–g)[37]. Moreover, the clinical relevance of the CtBP-targeted gene list is further supported by analysis of two independent breast cancer gene expression studies revealing that patients, whose tumors can be classified as showing differential expression of CtBP-target genes, have significantly shorter metastasis free survival by Kaplan-Meier analysis (Fig. 5c).

High CtBP predicts poor survival in breast cancer patients

The data presented thus far suggests that CtBP is likely to play a substantial role in the etiology and progression of human breast cancer. To examine CtBP expression in patient tissues, tumor samples from two independent breast cancer cohorts were stained for CtBP protein expression by immuno-histochemistry using antibodies against CtBP (Fig. 6a). In normal breast CtBP, nuclear immuno-reactivity is generally light and non-uniform with many nuclei showing little or no CtBP staining, while in patients with basal-like, triple-negative breast cancer, CtBP1 staining is much more intense (Fig. 6a). When digitally scored for CtBP nuclear staining to measure percent of nuclei with scores of 0–3 (nuclear intensity) or a score weighted by nuclear size (nuclear score), triple negative breast cancer shows a nuclear intensity and nuclear score that is 25 and 22 times higher than normal breast respectively (Fig. 6a). This system was then used to score the first patient tissue cohort (the training set) (Fig. 6b). When this scoring system was used to segregate patient samples into 3 groups of low (nuclear score <100; nuclear intensity <2); medium (nuclear score 100–300; nuclear intensity 2–5) and high (nuclear score >300; nuclear intensity >5) CtBP score, there was a clear trend showing an inverse relationship between CtBP staining and patient median survival by Kaplan Meier analysis (Fig. 6b). Using the same parameters these trends were reproducible in a second independent cohort (Patient validation set) of equivalent size (Fig. 6c). This suggests that elevated CtBP can function as a surrogate biomarker for altered epigenetic regulation in breast cancer patients who may progress to more advanced disease.

Reversal of CtBP function by small molecule Inhibition

CtBP is a potent epigenetic regulator that responds to cellular metabolism through its interaction with NADH. Therefore, pharmacological targeting of CtBP may, in principle, provide a means of derepressing its transcriptional targets. Though CtBP is a member of the d-2-hydroxyacid dehydrogenase family, its true substrate is not known [38]. Recent studies indicate that 2-Keto-4-methylthiobutyrate (MTOB), an intermediate in the methionine

salvage pathway, can bind CtBP and reverse repression of the proapoptotic gene, *BIK*, in colon cancer cells [39, 40]. To test if MTOB could disrupt expression of CtBP target genes in breast cancer, both MCF-7 and MDA-MB-231 were incubated in the presence and absence of MTOB and the 30 CtBP targeted genes (Fig. 1b) were screened for changes in gene expression (Figs. 7a–b and Supplementary Fig. S13), and promoter occupancy (Figs. 7d–e and Supplementary Figs. S14–S15). MTOB treatment caused significant derepression ($P<0.05$) of 40% of these genes in MCF-7 and 46% in MBA-MD-231. Approximately 3% and 10% of genes, respectively, were repressed (Figs. 7a–b and Supplementary Fig. 13). The concordance of the MTOB effect between the two cell lines was 70% (21/30) indicating that MTOB action is relatively independent of breast cancer subtype and epithelial programming (Fig. 7b and Supplementary Fig. S13). However, though it is difficult to know the extent to which this derepression is due to direct targeting of CtBP occupancy or to indirect effects; incubation with MTOB caused a significant displacement ($P<0.05$) of CtBP from 67% of the promoters in MCF-7 and only 30% from promoters in MDA-MB-231 (Fig. 7d and Supplementary Fig. S14). The lower MTOB-induced CtBP displacement in MDA-MB-231 could be due to the lower level of CtBP binding found at these genes (Supplementary Fig S3). This could explain, in part, why the concordance between changes in CtBP occupancy and gene expression is significantly higher for MCF-7 (>70%) compared to MDA-MB-231 (50%) following MTOB treatment (Figs. 7a–d and Supplementary Figs. S13–S15). Nonetheless, these data suggest that the predominant mode of MTOB action is through its eviction of CtBP from occupied promoter regions. Finally, treatment with MTOB antagonizes the mesenchymal phenotype (Figs. 7e–f). Addition of MTOB to both MCF-7 and MDA-MD-231 increases the pro-epithelial *E-cadherin/Vimentin* ratio while reducing the pro-mesenchymal CD44/CD24 ratio, with a more significant trend ($P<0.05$) in MCF-7 (Figs. 7e–f). Taken all together, these findings provide substantial evidence that pharmacological targeting of CtBP to disrupt malignant cellular reprogramming may be a feasible “epigenetic strategy” for therapeutic intervention.

Discussion

The evidence of a link between obesity and diabetes and increased mortality from breast cancer is incontrovertible [41–44]. An important feature of the dysfunctional energetics associated with obesity and diabetes and malignant transformation, is elevated carbohydrate metabolism, a central component of the Warburg Effect [45, 46]. This elevated level of carbohydrate metabolism, whether due to the over-nutrition of obesity or the Warburg Effect of cancer bioenergetics, results in increased levels of NADH [47–49]. In this study we propose CtBP is a key downstream epigenetic effector of elevated NADH. Therefore through CtBP, changes in cellular metabolic status can drive genome-wide changes in chromatin through targeted recruitment of CtBP that facilitates the acquisition of epigenetically reprogrammed properties that promote genome instability, dedifferentiation, and the transformation to a more mesenchymal phenotype.

Though this study provides one of the first to profile the binding of CtBP throughout the mammalian genome; how, when, and where the different CtBP complexes target and coordinate the recruitment of specific chromatin modifiers, and their subsequent effect on the epigenome remain to be defined. These epigenetic networks and programs are likely to

differ by cellular process and cell type and are likely to reflect a hierarchy of CtBP complexes formed under specific cellular conditions and environments as we have seen in comparing the mesenchymal MDA-MB-231 cell line, with the luminal MCF-7 (Figs. 3, and 7). This difference has been demonstrated in prior studies where loss of CtBP had a much great effect on mitotic fidelity in MDA-MB-231 than MCF-7 [50]. Future studies to correlate global alterations in histone and DNA modification with changes in CtBP levels (via either genetic or metabolic disruption) in multiple breast cancer subtypes will be necessary to better define the mechanism underlying these differences.

Approximately 5–10% of breast cancers are secondary to inherited mutations of cancer predisposing genes. It is striking that, of the known and newly identified breast cancer predisposing genetic mutations, a substantial number are targeted for repression by CtBP, including *PALB2*, *BRIP1*, *RAD51C* and *BRCA1* [16]. Thus the observation that many patients develop breast cancers with features of inherited disease without demonstrating mutation in genes characteristic of the disease [51], is consistent with a role played by CtBP-regulated pathways in such tumors. Notably, decreased expression specifically of DNA repair proteins is associated with shortened time to recurrence in triple-negative breast cancer [52]. This is consistent with the demonstration, in this current study, of the impact of CtBP targeting on genome stability. Nearly one third of the Fanconi Anemia complementation group is targeted by CtBP. Therefore, it is not surprising that loss of CtBP expression or function results in a significant improvement in DNA repair in breast cancer cell lines (see Figs. 1d, and 2d–e). Most importantly, targeting by CtBP suggests that these hereditary risk factors for breast cancer may be worsened by lifestyle factors influencing metabolic imbalance.

Finally, many of the new driver mutations identified by recent systematic sequencing of cancer genomes has uncovered several genes with functional roles in epigenetic regulation [53]. CtBP represents a novel class of versatile, multi-potent epigenetic regulators that is likely to play many different roles in cancer etiology and progression. The finding that MTOB can act as a small molecular inhibitor that can reverse genomic targeting by CtBP, provides a proof of principle that pharmacological manipulation of CtBP is feasible. Thus epigenetic targeting through CtBP promises to be a new and exciting area of future therapeutic intervention. New efforts will have to be directed at finding compounds that will function in the nanomolar to micromolar range. Given that weight gain and obesity represent modifiable cancer risk factors linked to lifestyle, a better understanding of CtBP will fuel new ideas and creative strategies for combined behavioral and therapeutic approaches to cancer treatment and prevention.

Methods

Reagents

Hydrogen peroxide is from Invitrogen as 30% stock. MTOB (4-methylthio-2-oxobutyric Acid) is from Sigma-Aldrich and was dissolved in medium to 250mM and diluted to 10mM final concentration in cell culture. The antibody to CtBP used for ChIP was purchased from Santa Cruz Biotechnology and is cross-reactive with both CtBP1 and CtBP2. The anti-CtBP1 specific antibody and anti-CtBP2 specific antibody were purchased from BD

biosciences. Anti-acetylated histone H3, anti-acetylated histone H4 antibodies and anti-γH2AX antibody were obtained from Millipore.

Cell culture and tissues

Both MCF-7 cells and MDA-MB-231 cells were maintained in regular DMEM supplemented with 10% (v/v) FBS, penicillin-streptomycin (Invitrogen) and insulin. In addition, the regular DMEM has 4.5g/L glucose and is considered as high glucose culturing (HG) compare to 1.0g/L glucose DMEM medium(LG). The low glucose cultured cells were used for experiments only after 3 month of continuous culture in low glucose medium.

ChIP and ChIP-seq

All ChIP experiments were carried out as described [8]. The detailed procedure is provided in the Supplementary Methods.

ChIP-seq data analysis

The detailed ChIP-seq data analysis is provided in the Supplementary Methods. Briefly, the 36-mer short-read tags were mapped to the human genome (UCSC HG19). Enrichment of tags in a 250 bp target window relative to a 200 kb surrounding window (local background) was gauged by a model based on the binomial distribution. The hotspots are defined by a z-score calculated using the target window and the background window signals both centered on the tag. In addition, ChIP hotspots were refined into 150 bp peaks using a peak-finding procedure. The sequencing data from matching input samples are used for the processing of the ChIP data, as a measure of background signal.

Motif discovery and enrichment analysis

A motif discovery analysis was performed on selected DNA sequences using MEME [54] on parallel clusters at the NIH Biowulf supercomputing facility. DNA sequences for MEME input were from the top 1500 (by tag density) hotspots among all CtBP binding hotspots. To limit the computational load, only the 200 bp regions with the highest tag density were used instead of the entire width of a hotspot in cases where the hotspot spanned greater than 200 bp. The width of motifs to discover was set to 6 and 20 for minimum and maximum, respectively. To identify motifs for known transcription factor binding, individual position-specific probability matrices against the Transfac database were queried using the TomTom software (http://meme.nbcr.net/meme/cgi-bin/tomtom.cgi). Statistically significant matches were retrieved that share the majority of specific nucleotides in the sequence motifs. To generate consensus read densities for positions relative to transcription start sites (TSS), the total number rd* of read tags summed over all Refseq annotated TSS normalized to the length L of the genome and the total number N of aligned reads (rd* = rd* L/N) was profiled such that rd*=1 approximately corresponds to an un-enriched distribution of reads.

Gene expression and Microarray analysis

The total RNA from 3 biological replicates of control MCF-7 cells and CtBP knockdown MCF-7 cells were prepared using the RNAeasy kit (Qiagen) following the manufacturer's protocol. Synthesis of cDNA from total RNA and hybridization/scanning of microarrays

were performed with Affymetrix GeneChip products (HGU133plus2) as described in the GeneChip manual. Raw data files (.CEL) were converted into probe set values by RMA normalization. Following RMA-normalization, Bioconductor packages was applied in R statistical environment to generate a list of genes that are differentially expressed between control cells and CtBP knockdown cells and $p<0.05$ was considered as significant. The data was stored as NCBI GSE36529.

Comet assay

Comet assays were performed according to Olive et al 2006 [55]. Briefly, a single-cell suspension was prepared using enzyme disaggregation. The cells were exposed to neutral lysis buffer (2% sarkosyl, 0.5M Na_2EDTA, 0.5 mg/ml proteinase K (pH 8.0); equilibrated at 4 °C) for overnight at 37°C. Following electrophoresis the cells were stained by SYBR Green and the images were obtained using fluorescent microscopy. The tail moment was calculated by the following formula: Tail moment=tail length x percentage of Tail DNA. Percentage of Tail DNA= aT×iT/(aT×iT+aH×iH), where aT = the tail area, iT = average intensity of tail, aH = the head area and iH = average intensity of Head. Comet Score™ was used to analyze the comet pictures.

Immunofluorescence staining of cells

Cells were grown on cover-slips and fixed in 3.5% paraformaldehyde. For γH2AX staining the cells were incubated with Alexa Fluor® 488 Goat Anti-Mouse IgG for 1hr. Cells were irradiated at 10 Gy to induce DNA damage.

Immunohistochemistry staining of tissues

Detailed methods for immunohistochemistry is provided in the Supplementary Methods. Formalin-Fixed, Paraffin-Embedded (FFPE) tissues were de-paraffinized by submerging the slides in Xylene. Antigen retrieval was performed in buffers containing 100mL of 1mM EDTA pH 8.0. Staining was developed using secondary antibody conjugated with horse-radish peroxidase (HRP) (Dako EnVision + System-HRP Labelled Polymer Anti-Rabbit or Anti-mouse and counterstained with hematoxylin.

Analysis of Tissue Microarrays

Immunohistochemically stained tissue slides were converted to digital slide images by scanning the slides on an Aperio ScanScope XT slide scanner. High resolution digital slide images were then archived into Aperio's digital pathology information management system "Spectrum". Digital slide images were analyzed using Aperio's IHC Nuclear Image Analysis algorithm to assess the nuclear staining for CtBP in MCF7 cells and quantify the intensity of individual cells. Values and colors are assigned to individual cells based on the intensity of nuclear staining with a classification of 0 (blue), 1+ (yellow), 2+ (orange) and 3+ (red). Nuclear intensity was calculated from the sum of the product of the % of cells with 3+ and 2+ scores divided by the sum of the product of % cells with 1+ and 0 scores. Nuclear score was calculated as the product of nuclear area (um^2) and the nuclear intensity. Archival FFPE tissues from breast cancer patients were obtained from the surgical pathology archive of the University of Chicago for tissue microarray (TMA) construction. The study was

approved by the Institutional Review Boards University of Chicago and East Carolina University. Pathological features, including histological diagnosis, grade, tumor size, and axillary lymph node metastasis, were abstracted from the pathology report. There were survival data on 98 to 100 breast cancer patients from each data set with a median follow-up of 8.3 years.

Analysis of Breast Cancer Gene Expression Profiles

Expression patterns of the 1,823 genes identified by CtBP ChIP-Seq were examined in a previously published breast cancer containing microarray and patient clinical data set available from the University of North Carolina (UNC) which includes 337 human breast tumors (UNC337) and is available in the Gene Expression Omnibus (GEO) under accession number GEO:(GSE18229) [10]. All data sets were median centered within each data set and standardized to zero mean and unit variance before downstream analysis [10]. ANOVA analysis of representative gene expression in tumor samples was determined using the UNC337 gene expression dataset. To determine if the overlap of CtBP target gene lists with other referenced gene lists, is statistically significant in Venn Diagrams, a hypergeometric distribution was calculated to derive the statistical P-value based on 37630 TSSs in refseq (HG19, USCS). Analysis of patient survival associated with gene expression from breast cancer datasets was performed using BRB ArrayTools Version: 4.1.0 - Beta_3 Release. Affymetrix data sets were downloaded from the NCBI Gene Expression Omnibus (GEO; http://www.ncbi.nlm.nih.gov/geo/). Expression data were loaded into BRB ArrayTools using the Data Import Wizard. U133A probe sets for the individual gene signatures were identified by using the Affymetrix NetAffx Analysis Center Batch Query tool (http://www.affymetrix.com/analysis/index.affx). Expression data were filtered to exclude any probe set that was not a component of the signatures tested, and to eliminate any probe set whose expression variation across the dataset was P>0.05. Kaplan-Meier analysis was performed using the Survival Risk Prediction tool, specifying two risk groups, with fitting to a Cox proportional hazard model with p-value ≤ 0.05. Distributions of the hazard ratios and the logrank test P-values was determined based on 1000 Bootstrap samples where each bootstrap sample consists of 50% of cases randomly selected from the whole set [56].

Statistical analysis

All the error bars represent the standard deviations of the mean from at least 3 independent biological replicates unless otherwise indicated. Comparison between two groups was done using a 2-sided Student's t test. P-value<0.05 was considered statistically significant.

Supplementary Material

Refer to Web version on PubMed Central for supplementary material.

Acknowledgments

This research was supported by the Intramural Research Program of the US National Institutes of Health, the US National Cancer Institute, the US National Institute on Aging, and the US National Institute on Minority Health and Health Disparities.

References

1. Hanahan D, Weinberg RA. Hallmarks of cancer: the next generation. Cell. 2011; 144:646–674. [PubMed: 21376230]
2. Vogelstein B, Kinzler KW. Cancer genes and the pathways they control. Nat Med. 2004; 10:789–799. [PubMed: 15286780]
3. Baylin SB, Jones PA. A decade of exploring the cancer epigenome -biological and translational implications. Nat Rev Cancer. 2011; 11:726–734. [PubMed: 21941284]
4. Ram O, et al. Combinatorial patterning of chromatin regulators uncovered by genome-wide location analysis in human cells. Cell. 2011; 147:1628–1639. [PubMed: 22196736]
5. Chinnadurai G. The transcriptional corepressor CtBP: a foe of multiple tumor suppressors. Cancer Res. 2009; 69:731–734. [PubMed: 19155295]
6. Zhang Q, et al. Redox sensor CtBP mediates hypoxia-induced tumor cell migration. Proc Natl Acad Sci U S A. 2006; 103:9029–9033. [PubMed: 16740659]
7. Zhang Q, Piston DW, Goodman RH. Regulation of corepressor function by nuclear NADH. Science. 2002; 295:1895–1897. [PubMed: 11847309]
8. Di LJ, Fernandez AG, De SA, Longo DL, Gardner K. Transcriptional regulation of BRCA1 expression by a metabolic switch. Nat Struct Mol Biol. 2010; 17:1406–1413. [PubMed: 21102443]
9. Perou CM, et al. Molecular portraits of human breast tumours. Nature. 2000; 406:747–752. [PubMed: 10963602]
10. Prat A, et al. Phenotypic and molecular characterization of the claudin-low intrinsic subtype of breast cancer. Breast Cancer Res. 2010; 12:R68. [PubMed: 20813035]
11. Mani SA, et al. The epithelial-mesenchymal transition generates cells with properties of stem cells. Cell. 2008; 133:704–715. [PubMed: 18485877]
12. Creighton CJ, et al. Residual breast cancers after conventional therapy display mesenchymal as well as tumor-initiating features. Proc Natl Acad Sci U S A. 2009; 106:13820–13825. [PubMed: 19666588]
13. Herschkowitz JI, et al. Comparative oncogenomics identifies breast tumors enriched in functional tumor-initiating cells. Proc Natl Acad Sci U S A. 2012; 109:2778–2783. [PubMed: 21633010]
14. Hildebrand JD, Soriano P. Overlapping and unique roles for C-terminal binding protein 1 (CtBP1) and CtBP2 during mouse development. Mol Cell Biol. 2002; 22:5296–5307. [PubMed: 12101226]
15. Valastyan S, Weinberg RA. Tumor metastasis: molecular insights and evolving paradigms. Cell. 2011; 147:275–292. [PubMed: 22000009]
16. Gage M, Wattendorf D, Henry LR. Translational advances regarding hereditary breast cancer syndromes. J Surg Oncol. 2012; 105:444–451. [PubMed: 22441895]
17. Wakano C, Byun JS, Di LJ, Gardner K. The dual lives of bidirectional promoters. Biochim Biophys Acta. 2012
18. DeSiervi A, et al. Transcriptional autoregulation by BRCA1. Cancer Res. 2010; 70:532–542. [PubMed: 20068145]
19. Kao J, et al. Molecular profiling of breast cancer cell lines defines relevant tumor models and provides a resource for cancer gene discovery. PLoS One. 2009; 4:e6146. [PubMed: 19582160]
20. Shi Y, et al. Coordinated histone modifications mediated by a CtBP co-repressor complex. Nature. 2003; 422:735–738. [PubMed: 12700765]
21. Wang J, et al. Opposing LSD1 complexes function in developmental gene activation and repression programmes. Nature. 2007; 446:882–887. [PubMed: 17392792]
22. Adamo A, et al. LSD1 regulates the balance between self-renewal and differentiation in human embryonic stem cells. Nat Cell Biol. 2011; 13:652–659. [PubMed: 21602794]
23. Wang Y, et al. LSD1 is a subunit of the NuRD complex and targets the metastasis programs in breast cancer. Cell. 2009; 138:660–672. [PubMed: 19703393]
24. Bhambhani C, Chang JL, Akey DL, Cadigan KM. The oligomeric state of CtBP determines its role as a transcriptional co-activator and co-repressor of Wingless targets. EMBO J. 2011; 30:2031–2043. [PubMed: 21468031]

25. McDonald OG, Wu H, Timp W, Doi A, Feinberg AP. Genome-scale epigenetic reprogramming during epithelial-to-mesenchymal transition. Nat Struct Mol Biol. 2011; 18:867–874. [PubMed: 21725293]
26. Loboda A, et al. EMT is the dominant program in human colon cancer. BMC Med Genomics. 2011; 4:9. [PubMed: 21251323]
27. Mortazavi A, Williams BA, McCue K, Schaeffer L, Wold B. Mapping and quantifying mammalian transcriptomes by RNA-Seq. Nat Methods. 2008; 5:621–628. [PubMed: 18516045]
28. Buijs JT, et al. BMP7, a putative regulator of epithelial homeostasis in the human prostate, is a potent inhibitor of prostate cancer bone metastasis in vivo. Am J Pathol. 2007; 171:1047–1057. [PubMed: 17724140]
29. Zhao LJ, Subramanian T, Vijayalingam S, Chinnadurai G. PLDLS-dependent interaction of E1A with CtBP: regulation of CtBP nuclear localization and transcriptional functions. Oncogene. 2007; 26:7544–7551. [PubMed: 17546044]
30. Chung CH, Bernard PS, Perou CM. Molecular portraits and the family tree of cancer. Nat Genet. 2002; 32 (Suppl):533–540. [PubMed: 12454650]
31. Turner N, Tutt A, Ashworth A. Hallmarks of 'BRCAness' in sporadic cancers. Nat Rev Cancer. 2004; 4:814–819. [PubMed: 15510162]
32. Cieply B, et al. Suppression of the epithelial-mesenchymal transition by Grainyhead-like-2. Cancer Res. 2012; 72:2440–2453. [PubMed: 22379025]
33. Werth M, et al. The transcription factor grainyhead-like 2 regulates the molecular composition of the epithelial apical junctional complex. Development. 2010; 137:3835–3845. [PubMed: 20978075]
34. Bernardo GM, et al. FOXA1 represses the molecular phenotype of basal breast cancer cells. Oncogene. 2012
35. Badve S, et al. FOXA1 expression in breast cancer--correlation with luminal subtype A and survival. Clin Cancer Res. 2007; 13:4415–4421. [PubMed: 17671124]
36. Subramanian A, et al. Gene set enrichment analysis: a knowledge-based approach for interpreting genome-wide expression profiles. Proc Natl Acad Sci U S A. 2005; 102:15545–15550. [PubMed: 16199517]
37. Charafe-Jauffret E, et al. Gene expression profiling of breast cell lines identifies potential new basal markers. Oncogene. 2006; 25:2273–2284. [PubMed: 16288205]
38. Kumar V, et al. Transcription corepressor CtBP is an NAD(+)-regulated dehydrogenase. Mol Cell. 2002; 10:857–869. [PubMed: 12419229]
39. Achouri Y, Noel G, Van SE. 2-Keto-4-methylthiobutyrate, an intermediate in the methionine salvage pathway, is a good substrate for CtBP1. Biochem Biophys Res Commun. 2007; 352:903–906. [PubMed: 17157814]
40. Straza MW, et al. Therapeutic targeting of C-terminal binding protein in human cancer. Cell Cycle. 2010; 9:3740–3750. [PubMed: 20930544]
41. Calle EE, Kaaks R. Overweight, obesity and cancer: epidemiological evidence and proposed mechanisms. Nat Rev Cancer. 2004; 4:579–591. [PubMed: 15286738]
42. Ewertz M, et al. Effect of obesity on prognosis after early-stage breast cancer. J Clin Oncol. 2011; 29:25–31. [PubMed: 21115856]
43. Sinicrope FA, Dannenberg AJ. Obesity and breast cancer prognosis: weight of the evidence. J Clin Oncol. 2011; 29:4–7. [PubMed: 21115867]
44. Taubes G. Cancer research. Unraveling the obesity-cancer connection. Science. 2012; 335:28, 30–28, 32. [PubMed: 22223787]
45. Vander Heiden MG, Cantley LC, Thompson CB. Understanding the Warburg effect: the metabolic requirements of cell proliferation. Science. 2009; 324:1029–1033. [PubMed: 19460998]
46. Koppenol WH, Bounds PL, Dang CV. Otto Warburg's contributions to current concepts of cancer metabolism. Nat Rev Cancer. 2011; 11:325–337. [PubMed: 21508971]
47. Yu Q, Heikal AA. Two-photon autofluorescence dynamics imaging reveals sensitivity of intracellular NADH concentration and conformation to cell physiology at the single-cell level. J Photochem Photobiol B. 2009; 95:46–57. [PubMed: 19179090]

48. Uppal A, Gupta PK. Measurement of NADH concentration in normal and malignant human tissues from breast and oral cavity. Biotechnol Appl Biochem. 2003; 37:45–50. [PubMed: 12578551]

49. Schwartz JP, Passonneau JV, Johnson GS, Pastan I. The effect of growth conditions on NAD+ and NADH concentrations and the NAD+:NADH ratio in normal and transformed fibroblasts. J Biol Chem. 1974; 249:4138–4143. [PubMed: 4369293]

50. Bergman LM, Birts CN, Darley M, Gabrielli B, Blaydes JP. CtBPs promote cell survival through the maintenance of mitotic fidelity. Mol Cell Biol. 2009; 29:4539–4551. [PubMed: 19506021]

51. Issa JP, Garber JE. Time to think outside the (genetic) box. Cancer Prev Res (Phila). 2011; 4:6–8. [PubMed: 21205738]

52. Alexander BM, et al. DNA repair protein biomarkers associated with time to recurrence in triple-negative breast cancer. Clin Cancer Res. 2010; 16:5796–5804. [PubMed: 21138871]

53. Stratton MR. Exploring the genomes of cancer cells: progress and promise. Science. 2011; 331:1553–1558. [PubMed: 21436442]

54. Bailey TL, Gribskov M. Methods and statistics for combining motif match scores. J Comput Biol. 1998; 5:211–221. [PubMed: 9672829]

55. Olive PL, Banath JP. The comet assay: a method to measure DNA damage in individual cells. Nat Protoc. 2006; 1:23–29. [PubMed: 17406208]

56. Li J, et al. Identification of high quality cancer prognostic markers and metastasis network modules. Nat Commun. 2010; 1:34. [PubMed: 20975711]

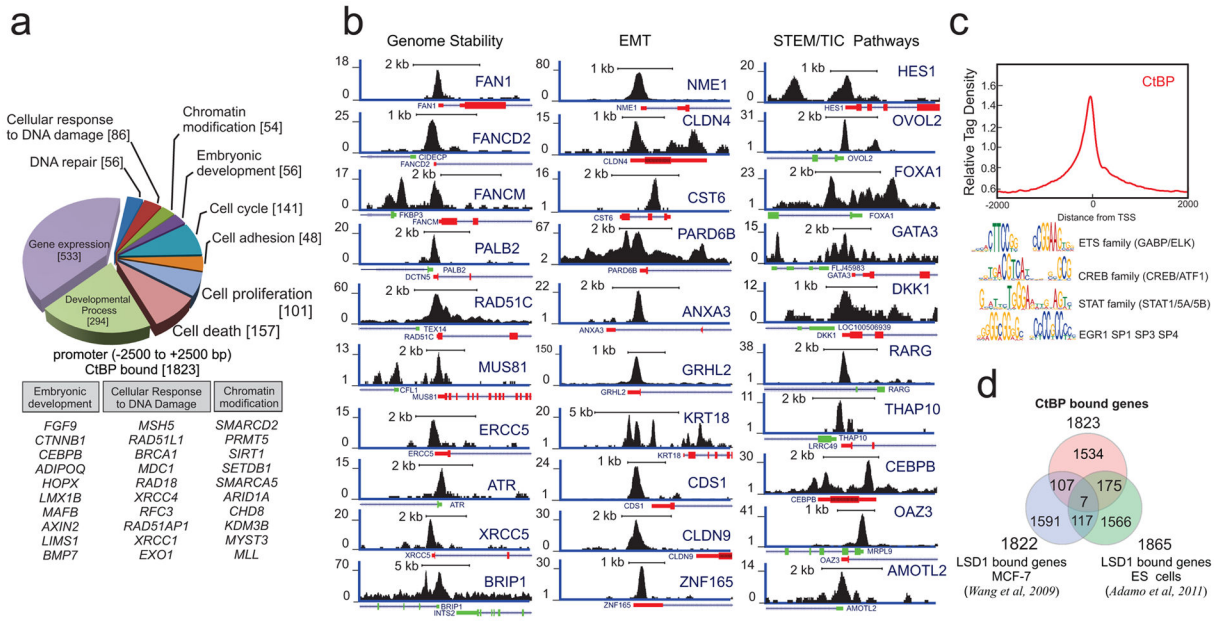

Figure 1.

Global targeting of genome stability and developmental pathways by CtBP differentiation (**a**) Gene ontology analysis indicates that CtBP targets numerous cancer related pathways linked to DNA repair, chromatin modifications, cell adhesion and other pathways important in developmental processes. (**b**) ChIP-Seq profiles of the binding of CtBP to selected genes that are key genetic drivers of human malignancy including genome stability, epithelial-to-mesenchymal transition (EMT) and stem cell/tumor initiation cell (TIC) pathways in MCF-7 cells. Red indicates genes encoded 5′-3′ on the upper strand while green indicates genes encoded 5′-3′ on the lower strand. (**c**) Binding motifs enriched under CtBP ChIP-seq peaks revealed by *in silico* analysis. (**d**) The large majority of promoter binding sites for CtBP are distinct from those bound by LSD1 in MCF-7 and human ES cells.

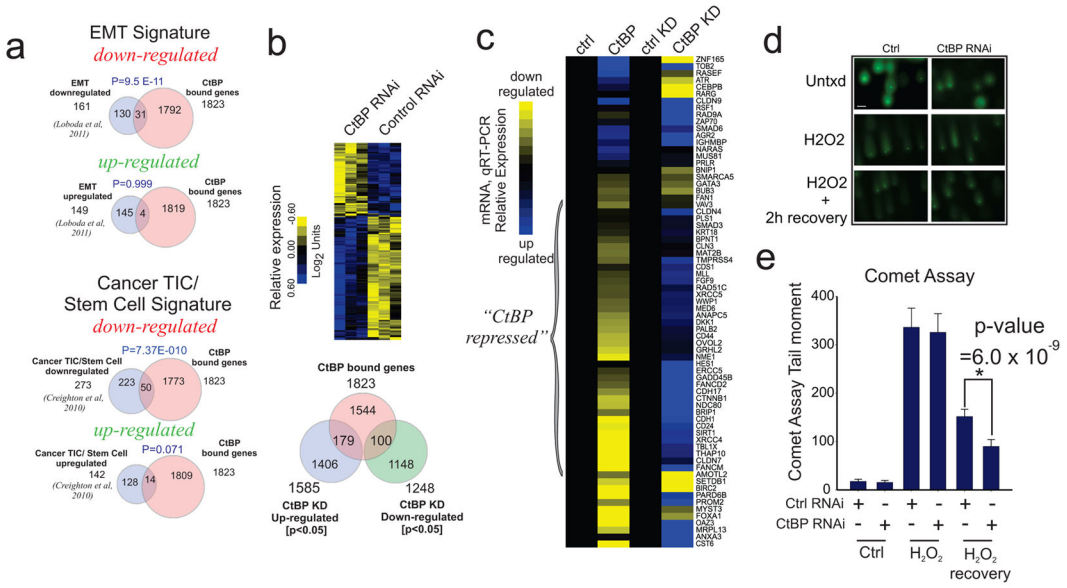

Figure 2. CtBP downregulated targets control differentiation and DNA repair

(**a**) Venn diagrams showing the overlap between CtBP targets and genes down-regulated and up-regulated in established EMT and Cancer tumor initiating cell (TIC)/stem cell gene signatures. P-values indicate the significance of overlap determined from hypergeometric distribution analysis. (**b**) Unsupervised hierarchical clustering of microarray analysis (HGU133plus) of differentially expressed (P<0.05) genes in control and MCF-7 cells depleted of CtBP by RNAi. Venn diagram shows the overlap of repressed and induced genes with CtBP targets identified by ChIP-seq. (**c**) Hierarchical clustering of the expression of multiple CtBP targets belonging to the gene classes, described in Figure 1, measured by quantitative real-time PCR in cells over-expressing CtBP (CtBP) and cells depleted of CtBP by RNAi (CtBP KD) compared to GFP control and non-targeting RNAi respectively. Bracket indicates CtBP repressed genes that were uniformly upregulated by CtBP depletion and repressed by CtBP overexpression. Corresponding expression values with error bars are provided in Supplementary Figures S4–S6 (**d**) Comet assay of MCF-7 cells before and after oxidative DNA damage by peroxide treatment and following 2 hour recovery in control cells and cells depleted of CtBP by RNAi. (**e**) Analysis of change in tail moment in control and CtBP depleted cells following DNA damage and recovery. The error bars represent the standard deviation of the mean from 2 independent experiments. Scale bar = 20 microns.

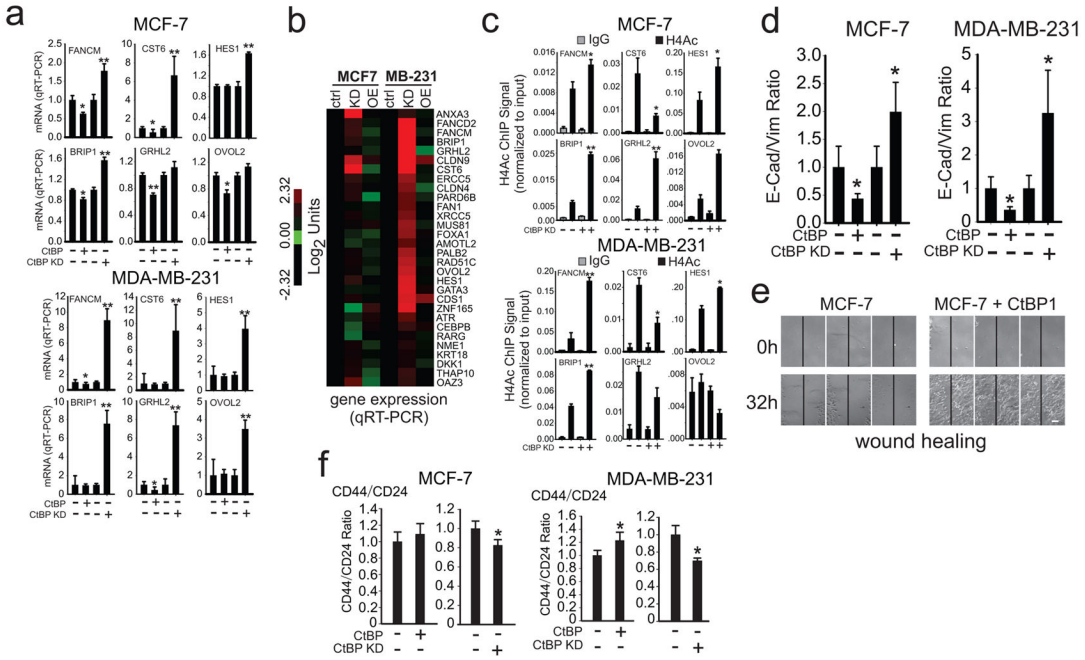

Figure 3. CtBP drives acquisition of mesenchymal traits in mammary epithelial cells

(**a**) Gene expression pattern of CtBP target genes controlling genome stability, EMT and Stem cell pathways in MCF-7 cells (top) and MDA-MB-231 cells (bottom) overexpressing CtBP or depleted of CtBP by RNAi as indicated. (**b**) Unsupervised hierarchical clustering comparing of the 30 gene validation set expression (see Figure 1b) in cells overexpressing or depleted of CtBP. Expression values with error bars are shown in Supplementary Figs. S4–S5. (**c**) Promoter Histone H4 acetylation profile (K5, K8, K12) of genes shown in (a) in MCF-7 cells (top) and MDA-MB-231 cells (bottom) following CtBP depletion by RNAi. Expression values and errors bars including the remaining 30 gene validation set are provided in Supplementary Fig S9. (**d**) E-Cadherin/Vimentin expression ratio in cells overexpressing CtBP or depleted of CtBP by RNAi. (**e**) Wound healing assay shows MCF-7 control cells and cells overexpressing CtBP1. Vertical line indicates center of wound in the scratch assay. White bar, 250 microns. (**f**) CD44/CD24 expression ratio in MCF-7 and MDA-MB-231 cells overexpressing CtBP or depleted of CtBP by RNAi. The error bars represent the standard deviation of the mean from 3 independent experiments (**a**, **d**, **f**) or 2 independent experiments (**c**). Single asterisk (*) indicates P <0.05) and double asterisk (**) indicates P<0.01.

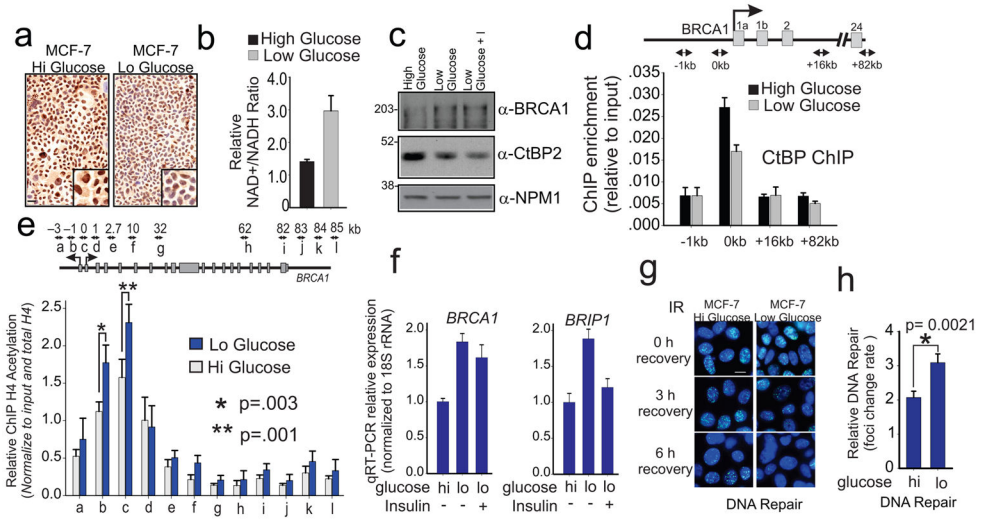

Figure 4. Calorie restriction decreases CtBP activity and increases DNA repair

(**a**) CtBP Immuno-histochemical staining of MCF-7 cells grown in high glucose (4.5 g/L) and lowglucose (1.0 g/L). Scale bar = 25 microns. Inset is 2 fold magnification. (**b**) NAD+/NADH ratio in lysates of MCF-7 cells grown in high and low glucose. (**c**) Western blot analysis of BRCA1 and CtBP2 expression in high and lowglucose treated cells. NPM1 was used as loading control. I= insulin. (**d**) ChIP profile of CtBP binding to the BRCA1 promoter in cells grown in high glucose versus low glucose as indicated. (**e**) ChIP profile of relative histone 4 lysine acetylation after normalization to ChIP for total histone 4. (**f**) qRT-PCR expression of *BRCA1* and *BRIP1* mRNA in high and low glucose treated cells with and without insulin. (**g**) phospho-gamma H2AX foci profile of cells following ionizing radiation at 0, 3 and 6 h. Scale bar = 10 microns. (**h**) Relative rate of DNA repair expressed as relative rate of decrease in foci per cell over time. The error bars represent the standard deviation of the mean from 3 independent experiments (**b**, **d**, **f, h**) or 5 independent experiments (**e**).

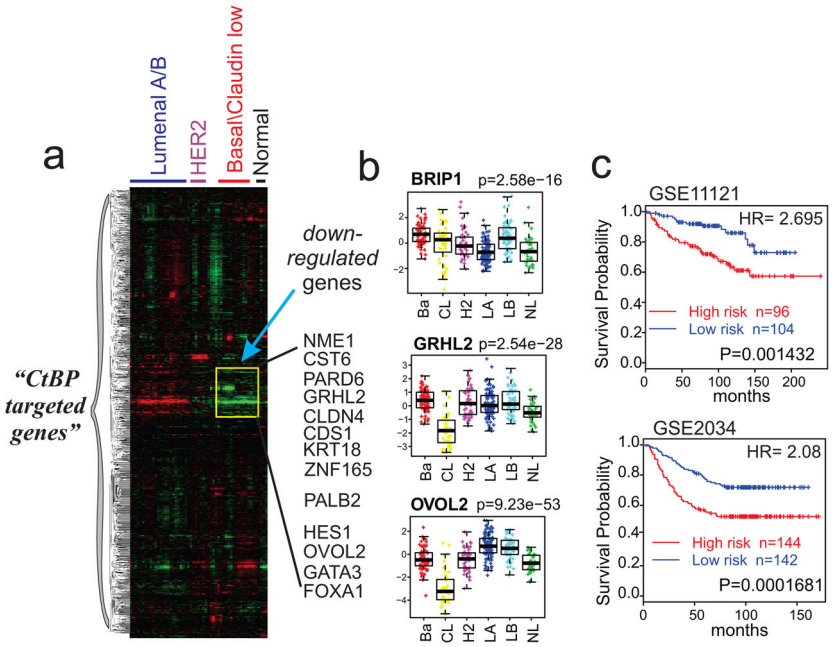

Figure 5. CtBP targets distinguish clinically aggressive subtypes of breast cancer

(**a**) Unsupervised hierarchical clustering of CtBP target genes in publically available breast cancer gene expression studies (UNC337). Highlighted rectangle indicates group of CtBP-bound genes that are downregulated/repressed preferentially in the basal-like subtype. (**b**) ANOVA profiling of one representative each of the genome stability (*BRIP1*), EMT (*GRHL2*) and TIC/Stem cell (*OVOL2*) gene groups, described in Figure 1b, using the UNC337 patient gene expression data set. P-values were calculated by comparing mean expression across all subtypes. (**c**) Patients whose tumors differentially express CtBP-bound genes show worse clinical outcome (metastasis-free survival) by Kaplan-Meier analysis. Patient gene expression data obtained from the Gene Expression Omnibus (GSE11121 and GSE2034) were separated into 2 groups based on differential expression CtBP target genes (red), and were analyzed by Kaplan Meier analysis. The 95% confidence interval for median HR=2.08 is [1.420, 3.070]. The 95% confidence interval for median HR= 2.70 is [1.490, 5.411]. P-values and hazard ratios (HR) were derived as described in materials and methods.

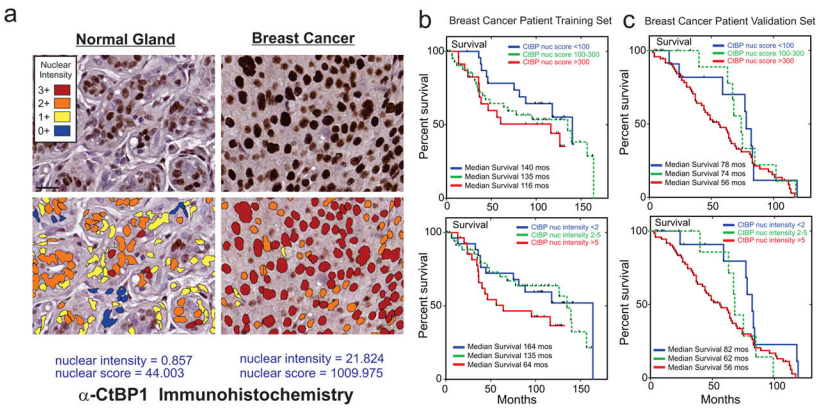

Figure 6. Eleveated CtBP protein in patient breast cancers predicts lower median survival

(**a**) CtBP1 immuno-histochemical staining of normal breast tissue and tissue from triple-negative breast cancer patients, analyzed for staining intensity using the Aperio nuclear algorithm software and then scored for nuclear intensity and nuclear score (weighted by nuclear area). Scale bar = 25 microns. (**b**) Relative survival of a training patient cohort (98) scored with low (<100 or <2.0), median (100–300 or 2–5) and high (>300 or > 5) scores for CtBP staining analyzed for survival trends by Kaplan-Meier analysis. Median survival for all 3 groups are shown. (c) CtBP scoring of a second independent breast cancer patient cohort (validation set) showing a similar inverse correlation between CtBP score and median survival.

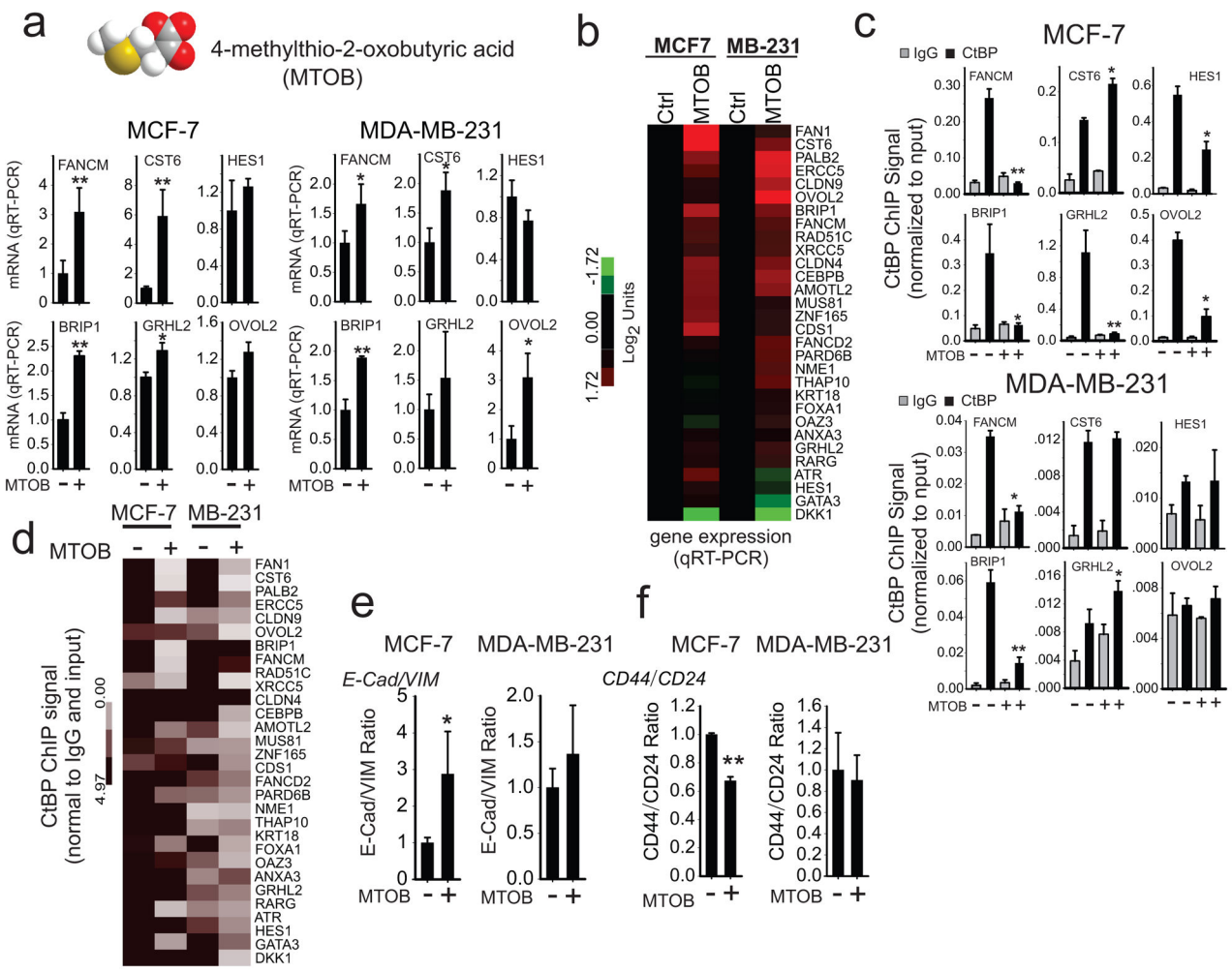

Figure 7. Small molecule inhibition reverses gene repression by CtBP eviction

(**a**) Gene expression pattern of CtBP target genes controlling genome stability, EMT and Stem cell pathways in MCF-7 cells (left) and MDA-MB-231 cells (right) with and without treatment with 10 mM MTOB. (**b**) Heat map of gene expression of the 30 gene validation set (Figure 1b) in MCF-7 (left) and MDA-MB-231 (right) cells treated with and without MTOB. Gene expression values and error bars including the remaining 30 genes are provided in Supplementary Fig. S13. (**c**) CtBP qChIP profiles of genome stability, EMT and Stem cell pathways genes in MCF-7 (top) and MDA-MB-231 (bottom) cells treated with or without MTOB. (**d**) Heat map of ChIP intensities of 30 gene validation list in MCF-7 and MDA-MB-231 cells treated with or without MTOB. Quantitative ChIP values and error bars are provided in Supplementary Fig. S14. (**e**) E-Cadherin/Vimentin ratio in MCF-7 and MDA-MB-231 cells treat with and without MTOB. (**f**) CD44/CD24 ratio in MCF-7 and MDA-MB-231 cells treat with and without MTOB.. The error bars represent the standard deviation of the mean from 3 independent experiments(**a**, **e**, **f**) or 2 independent experiments(**c**). Single asterisk (*) indicates P <0.05 and double asterisk (**) indicates P<0.01.

Table 1

Genome-wide binding sites for CtBP

Binding Site	# Sites
Promoter (<2.5 kB of TSS)	1823
Downstream peaks	916
Distal upstream peaks	1559
Intron	2056
Exon	253

Binding site distribution of CtBP in MCF-7 cells with Z-score ≥ 30. TSS= transcription start site.